



The mirabilite microbiocosm in a Carpathian contact cave

Oana Teodora Moldovan¹, Crin-Triandafil Theodorescu², Erika Andrea Level³, and Oana Cadar³

¹Emil Racovita Institute of Speleology, Romanian Academy – Cluj-Napoca Branch, 400006 Cluj-Napoca, Romania

²Museum Complex of Bistrița-Năsăud, 420016 Bistrița-Năsăud, Romania

³National Institute for Research and Development for Optoelectronics INOE 2000, Research Institute for Analytical Instrumentation Subsidiary, 400293 Cluj-Napoca, Romania

Correspondence: Oana Teodora Moldovan (oanamol35@gmail.com)

Received: 28 May 2025 – Discussion started: 1 August 2025

Revised: 25 May 2026 – Accepted: 26 May 2026 – Published: 26 June 2026

Abstract. This study examines the microbial and geochemical environment surrounding mirabilite (sodium sulfate decahydrate) deposits in Izvorul Tăușoarelor Cave, located in the Romanian Carpathians. Using a metabarcoding approach, we analysed mirabilite, sediments, dipluran insects, drip water, and moonmilk deposits to investigate the microbial communities and elemental profiles linked to mirabilite formation. Elemental analysis revealed a geochemical signature in mirabilite samples that was dominated by sodium, sulfur, and calcium. Microbial profiling revealed a unique pattern: sulfur-reducing bacteria, such as *Desulfobacterota*, were absent from mirabilite samples, whereas *Pseudomonas* dominated, suggesting an alternative sulfur cycling pathway that may involve sulfide biooxidation. The presence of ammonia-oxidising archaea (*Ca. Nitrocosmicus*) exclusively in the mirabilite area, and of bacteria (*Nitrococcus*), indicates a possible influence from a small bat colony, which contributes minimal ammonia that may support the microbial equilibrium required for mirabilite growth. *Actinomycetota*, abundant in mirabilite, may facilitate mineral crystallisation through mycelium-like structures. We propose the term “microbiocosm” to describe the interconnected network of biotic and abiotic elements surrounding the mirabilite environment and present a novel framework for investigating microbial contributions to its formation.

1 Introduction

Caves are restrictive habitats due to the lack of light, saturated air humidity, and relatively constant temperature. The absence of light, and consequently of plants, makes caves

and their associated subterranean habitats nutrient-deficient, with nutrients unevenly distributed across space and time (Howarth and Moldovan, 2018). However, in recent decades, autochthonous microorganisms have been proven to form the base of subterranean food chains, even in oligotrophic caves. These microorganisms can supply nutrients and essential enzymes, playing a crucial role in the adaptation and evolution of subterranean organisms.

In addition to supporting life in caves, cave microorganisms participate in the biogeochemical cycle of elements such as C, N, S, Fe, and Mn, as well as in mineral dissolution and precipitation processes (i.e., Banks et al., 2010; Koning et al., 2022; Zhu et al., 2022; Lange-Enyedi et al., 2024; Meka et al., 2024). These processes result in the deposition of carbonate speleothems, silicates, iron and manganese oxides, sulfur compounds, and nitrates. Such processes can be passive, with microbial cells acting as nucleation centres, or active, where bacteria produce enzymes involved in mineralisation or corrosion (dissolution).

A notable example in caves is the dissolution of limestone and precipitation of gypsum, which has been documented by various authors (see review in Northup and Lavoie, 2001). Microorganisms are also involved in the oxidation, reduction, and disproportionation of sulfur compounds, reactions that facilitate assimilation and produce energy. For example, *Thiobacillus* and *Desulfovibrio* decompose sulfur-containing amino acids and proteins, making sulfur available for organisms. The activity of these bacteria depends on environmental factors such as pH, temperature, and oxygen, which are crucial for sulfate mineralisation. Sulfur-oxidising bacteria and archaea catalyse processes that transform hydrogen sulfide and elemental sulfur into sulfate. Sulfate-reducing bac-

teria (*Desulfovibrio*, *Desulfobacter*) oxidise sulfate into the reduced state. Biodesulfurisation is driven by *Rhodococcus* and *Pseudomonas*, which can cleave sulfur-carbon bonds, thereby removing sulfur from organic compounds.

Next-generation techniques have provided an unprecedented understanding of the diversity and complexity of microorganisms in cave formations and mineralogical processes (i.e., De Mandal et al., 2015; Hershey and Barton, 2018; Zhu et al., 2021, 2022; Akacin et al., 2022; Haidău et al., 2022; Shen et al., 2022; Samanta et al., 2023).

Using metabarcoding, we propose a new approach to studying complex, microbe-driven interactions by integrating multiple living and non-living elements to investigate mirabilite, a rare and elusive cave mineral. Mirabilite is a sulfate mineral that forms monoclinic crystals of hydrated sodium sulfate ($\text{Na}_2\text{SO}_4 \cdot 10\text{H}_2\text{O}$) and usually deposits in salt lakes. Mirabilite, also known as Glauber's salt (Hill, 1979), was used in traditional medicine (Tao et al., 2024) and even mined by prehistoric populations from several areas within the Mammoth Cave System (USA; White, 2017).

It is an unstable mineral that can quickly lose water molecules and form thenardite, which remains unaltered in cold, shallow marine environments (Azzaro et al., 2022). Thenardite forms under warmer conditions and at temperatures below 10 °C; its hydration yields mirabilite (Marliacy et al., 2000). Therefore, cold air and humidity, as in caves, are the prerequisites of mirabilite maintenance. It has been identified in several caves around the globe, particularly in the Northern Hemisphere (White, 2019), and in lava tubes at higher altitudes (White, 2010; Mulder et al., 2023).

The hydrated sulphates of magnesium and sodium have raised attention for their use as analogues for water availability on other planets (Puławska et al., 2021). Microbial cells and associated beta-carotene in fluid inclusions within mirabilite suggest that these may be places to search for life in Mars samples (Gill et al., 2023) or evidence of groundwater (Möhlmann and Thomsen, 2011; Battler et al., 2013).

Bacteria-induced mineral precipitation (BIMP) is the process by which bacterial activity promotes mineral formation indirectly through metabolic by-products and surface interactions with ions (Bazyłinski et al., 2007; Hoffmann et al., 2021). Microorganisms can play a role in the formation and transformation of mirabilite in saline and sulfate-rich environments. While mirabilite primarily precipitates through abiotic evaporation and cooling, microbial activity can indirectly influence its formation by altering the geochemical conditions. Microbial communities in soil or water decompose organic matter and release sulfate through oxidation, thereby contributing to the sulfate pool available for mirabilite precipitation. Bacteria, such as *Desulfovibrio* and *Desulfobacter*, reduce sulfate (SO_4^{2-}) to sulfide (S^{2-}), thereby depleting sulfate from the solution and affecting local chemical equilibria. This can impact mirabilite precipitation by affecting its supersaturation in brine environments. Therefore, even if mirabilite is abiotic, microorganisms are

involved in its formation by modifying sulfate availability through metabolic activity, acting as nucleation sites for crystal growth, and creating local chemical conditions to favour precipitation.

In this study, we aimed to analyse the microbiome of the mirabilite substrate in a Romanian cave (Eastern Carpathians) by examining the bacteria diversity in comparison with cave sediments in areas without mirabilite, as well as in water and among the living organisms predominantly found around the mirabilite. Our unique approach is based on the concept of this mineral's microbiocosm, which is relatively uncommon in caves. To understand the mirabilite microbiocosm, we compared several microhabitats within the cave by incorporating the microbiomes of the living organisms. The results are primarily expressed as the presence or absence of microorganisms in each microhabitat, and why mirabilite forms only in small spots within a single room inside the cave. The results contribute to a deeper understanding of microorganism involvement in mirabilite formation and enhance knowledge of how this unique mineral affects or inhibits the survival of invertebrates in cave conditions, providing insights into potential analogues on other planets.

2 Materials and Methods

2.1 Cave description

Izvorul Tăușoarelor Cave (Tausoare Cave) is situated in northern Romania, within the Rodnei Mountains, at an elevation of 942 m above sea level (Fig. 1a). The cave measures 8.65 km in length and reaches a depth of 409 m. It is formed within a narrow strip of sandy Upper Eocene (Priabonian)-Lower Oligocene (Rupelian) limestone, interbedded with thin layers of black bituminous shale (Onac et al., 2019). Fine-grained pyrite is dispersed throughout the limestone and shale. These 60 m-thick karstic formations (Silvestru and Viehmann, 1982) lies above a Middle Eocene conglomerate bed that rests on the crystalline basement of the Rodnei Mountains (Kräutner et al., 1989).

The water that enters the cave sinks ~300 m upstream of the entrance and flows through various cave passages, resurfacing 5.7 km from the cave terminus (Viehmann et al., 1964).

The cave's mean annual temperature ranges from 6.5 to 8 °C, humidity is consistently 100 % in its deepest parts (Table 1), and air CO_2 levels are 470 ppm throughout the cave.

The cave "center" is Sala de Mese (Tables Room) from where many other passages like the Gypsum Gallery and rooms (Balls Room) continue (Fig. 1b). The Gypsum Gallery also gave the cave its fame for the unique gypsum speleothems (anthodites, crusts and crystals; Fig. 1). The primary source of sulphate ions is from the oxidation of pyrite in limestone and bituminous shale, as well as the overlying sandstone (Onac et al., 2019). Mirabilite is present in the Ta-

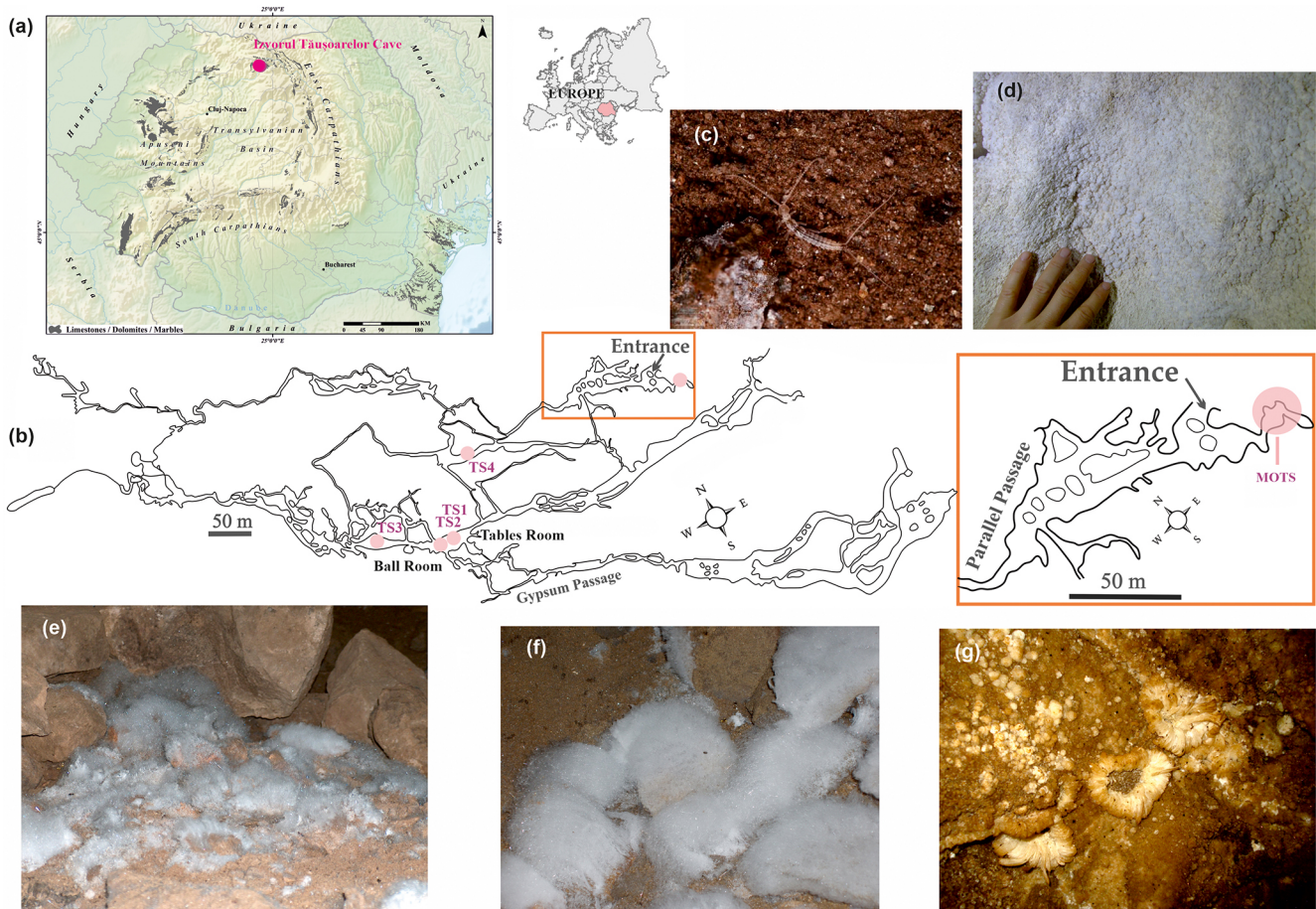


Figure 1. Izvorul Tăușoarelor Cave localisation and sampling points. (a) Position of the cave in northern Romania (south-east Europe); (b) Sampling stations inside the cave (see Table 1 for abbreviations); (c) Endemic dipluran *Litocampa humilis comani* (Insecta); (d) Moonmilk; (e) Mirabilite on a sediment heap; (f) Detail of the mirabilite; (g) Anthodites in the Gypsum Passage. Map modified after Onac et al. (2019), photos (c), (d), (e), and (f) by CTT, photo (g) by Traian Brad.

bles Room as patches of fine, white, needle-like crystals that occasionally disappear (Fig. 1e–f). Its presence, along with other minerals such as arcanite, epsomite, syngenite, leonite, and konyaite, is associated with reactions between slightly acidic karstic water and Ca, Na, K, and Mg anions from limestone, sandstone, and clay.

The cave was declared a scientific reserve in 1965 and is currently classified with the highest level of protection afforded to a cave under Romanian legislation.

2.2 Samples description

We collected two mirabilite samples from the cave, specifically from the Tables' Room (sampling stations TS1 and TS2, as shown in Fig. 1b).

One moonmilk sample was taken from a side passage near the cave entrance (MOTS, Fig. 1B and D). The sampling site is a cave wall coated with a moonmilk layer of variable thickness (analysis of this sample is presented in Theodorescu et al., 2023). Moonmilk is a whitish, carbonatic cave deposit,

with abiotic and biotic processes supposedly involved in its formation (Barton and Northup, 2007; Baskar et al., 2011; Dhimi et al., 2018). Different stages in bacteria's moonmilk formation are correlated with distinct structures and fabrics in crystal morphology (Canaveras et al., 2006).

Sediment samples were collected from the immediate vicinity of the mirabilite heap (STS1) and approximately fifty meters away (STS2), as shown in Fig. 1b, from the Ball Room (STS3), and dripping water in an active passage (WTS4).

For a comprehensive view, we added the moonmilk sample and the microbiome of 10 dipluran (Insecta) individuals. The diplurans were found next to the mirabilite heap in Station 2 and in the next room, the Balls Room, in Stations 3 and 4 (Fig. 1).

The only insect adapted to caves (troglobiont) and endemic to this cave, found in relatively high abundance in the Tables Room, is the dipluran (Insecta) *Litocampa humilis comani* Condé, 1991 (Fig. 1c). Individuals are frequently found

around the mirabilite heap, on the sediments. We collected data from 10 individuals (4 from TS2 and 6 from TS3), with TS3A and TS3B located a few meters apart.

2.3 Physicochemical Analysis

The mirabilite, moonmilk, and sediment samples were dried in air, ground into a fine powder, and sieved through a 100 μm -mesh steel sieve for chemical analysis. The pH and electrical conductivity (EC) were measured in water and a 1/5 solid-to-water suspension using a Seven Excellence multiparameter 130 (Mettler Toledo). Three grams of solid samples were dissolved in 21 mL of a 3 : 1 (*v/v*) mixture of HCl (30 %) and HNO₃ (65 %) in a sand bath. Dripping water samples were filtered and acidified with 2 drops of HNO₃ (65 %) before analysis. Na, Mg, K, Ca, Al, Fe, S, and P concentrations were measured using inductively coupled plasma optical emission spectrometry (ICP-OES) with a 5300 Optima DV (PerkinElmer, USA) spectrometer equipped with a pneumatic nebuliser. The concentrations of V, Cr, Mn, Co, Ni, Cu, Zn, Cd, Pb were measured by inductively coupled plasma mass spectrometer (ICP-MS) using an Elan DRC II (Perkin Elmer, USA) spectrometer in standard operation (Dynamic Reaction Cell in rf only mode). The concentration of water-soluble sulfates was measured in a 1/10 solid-to-water extract using a 761 Compact ion chromatograph (Metrohm) and converted into water-soluble S by multiplying the concentration of water-soluble sulfates by 0.33. The presence of carbonate and sulphate groups was identified by Fourier-transform infrared (FTIR) spectroscopy of dried and powdered samples, using a Spectrum BX II (Perkin Elmer) instrument equipped with an attenuated reflectance accessory (PIKE Technologies). The presence of carbonate and sulfate groups was analysed by Fourier-transform infrared spectroscopy using a Spectrum BX II (Perkin Elmer) instrument equipped with an attenuated reflectance accessory. X-ray diffraction measurements were performed using a Bruker D8 Advance XRD (Bruker) diffractometer with CuK α radiation ($\lambda = 1.5418 \text{ \AA}$) operating at 40 kV and 40 mA. Semi-quantitative analysis was conducted using the reference intensity ratio (RIR) method.

2.4 DNA Extraction

Before genomic DNA extraction, cells were disrupted using FastPrep-24TM (MP Biomedicals). DNA extraction was performed using the commercial Quick-DNA Fecal/Soil Miniprep kit (Zymo Research) according to the manufacturer's protocol. Furthermore, DNA quantification was performed using the SpectraMax QuickDrop (Molecular Devices). Triplicate sub-samples were analysed for each sample.

The extracted DNA was used as a template to investigate the composition of microbial communities and was sent for 16S rRNA metagenome sequencing using a commercial ser-

vice provider MacroGen Europe. PCR of the V3-V4 hyper-variable regions of the bacterial and archaeal SSU rRNA gene (Herlemann et al., 2011) was performed according to Illumina's 16S amplicon-based metagenomic sequencing protocol using the universal primers 341F and 805R.

2.5 Metabarcoding Analysis

Reads with a minimum length of 250–300 nt were analysed; Cutadapt v2.9.30 was used to remove sequencing primers and reads with N characters. Furthermore, the DADA2 package (Martin, 2011), implemented in R by adapting an existing pipeline (Callahan et al., 2016a), was used to process paired-end reads from all samples, enabling precise differentiation between actual biological variation and sequencing errors. After primer removal, the resulting paired ends were loaded into the DADA2 pipeline, trimmed, filtered, and merged with a minimum required overlap of 50 nt. Chimeras were removed from merged pairs. Curated ASVs (amplicon sequence variants) were taxonomically classified using SILVA 138.1 database (Callahan et al., 2016b).

From the obtained ASVs, the mean value of triplicate sub-samples was used in the subsequent analysis.

Sequence data generated in this study have been deposited in the European Nucleotide Archive (ENA) under the accession number PRJEB63212 for moonmilk and the rest of the samples in the National Centre for Biotechnology Information (NCBI) under accession number PRJNA1259755.

2.6 Statistical Analysis

The Phyloseq package in R (McMurdie and Holmes, 2013) was used to process community composition and statistical differences. Mean values of replicated samples were calculated to merge them, followed by Bray-distance-based hierarchical clustering and alpha-diversity analysis. The `tax_glom` function in phyloseq (Pruesse et al., 2007) was used to perform taxonomic agglomeration, generating counts and relative abundances at the genus, family, and phylum levels. Only 10 counts in at least one averaged sample were considered for abundance estimation for taxa merged at each taxonomic rank.

Principal Components Analysis (PCA) was used to represent the relationships among bacterial abundances across samples. Agglomerative Hierarchical Clustering (AHC), based on dissimilarities and Euclidean distances, was used to cluster bacterial abundances across samples. Multidimensional Scaling (MDS) for the samples in a 2-dimensional space based on their physicochemical similarities. For the MDS, a similarity matrix was generated using Pearson correlation as the proximity measure among the physicochemical parameters. Stress is a goodness-of-fit measure that ranges from 0 to 1, with values near 0 indicating a better fit. The analysis was done in XLSTAT 2024.4.1.

Table 1. Analysed samples from Tausoare Cave.

Type	Station Code/Date	Temperature (°C)	Relative air humidity RH (%)
Mirabilite	MTS1dec	7.0	100
Mirabilite	MTS2dec	7.0	100
Sediments	STS1mar	7.0	100
Sediments	STS2mar	7.0	100
Sediments	STS1sep	7.2	100
Sediments	STS2sep	7.2	100
Sediments	STS3Asep	8.0	100
Sediments	STS3Bsep	8.0	100
Dripping water	WTS4mar	2.7	–
Dripping water	WTS4sep	7.1	–
Moonmilk	MOTSmay	7.7	90
Diplura microbiome	Lit_TS2mar	7.0	100
Diplura microbiome	Lit_TS2sep	7.2	100
Diplura microbiome	Lit_TS3Asep	8.0	100
Diplura microbiome	Lit_TS3Bsep	8.0	100

Alpha diversity indices, Shannon, and Chao1, used to describe sample composition were calculated in PAST ver. 5.3.

3 Results

3.1 The mirabilite bacteriocosm

In the mirabilite samples, we obtained between 65 985 and 95 523 reads, and the samples were directly compared. One identified ASV represented *Crenarchaeota*, and 176 ASVs belonged to *Bacteria*. *Pseudomonadota* (84 % and 53 %) and *Actinomycetota* (10 % and 12 %) were the dominant phyla in both samples. It was followed by *Bacteroidota*, abundant only at Station 2 (~ 7 %). *Gemmatimonadota*, *Bacillota*, and *Chloroflexota* followed in lower abundances in one or both stations (Fig. 2a). *Gammaproteobacteria* were the most abundant class in both samples (82 % and 50 %), followed by *Actinobacteria* and *Bacteroidia* in Station 2, and *Acidimicrobiia* in Station 1. *Pseudomonas* was the most abundant genus in both samples (mean value 55 %), followed by *Lysobacter* (14 %) in Station 2 and an unassigned *Actinomarinales* in Station 1 (5.7 %; Fig. 2a).

The five sediment samples contained 455 Bacterial ASVs and 8 Archaeal ASVs, except Station 3, where mirabilite was absent. *Pseudomonadota* was the most abundant phylum in all the sediment samples (mean value 49 %), followed by *Gemmatimonadota* (~ 17 %) and *Bacteroidia* (~ 10 %) only in some of the samples (Fig. 2c). *Actinomycetota*, *Acidobacteriota*, and *Bacillota* were also abundant in some of the samples. *Gammaproteobacteria* was the dominant class in all the sediment samples, with a mean abundance of 45 %, followed by *Longimicrobia* and *Bacteroidia*. *Bacteroidia* were abundant only in the September sediment samples. *Lysobacter* was abundant in all sediment samples (~ 33 %; Fig. 2c) but

not *Pseudomonas*. Following in abundance were the unassigned *Longimicrobia* and *Anseongella*.

Moonmilk composition was discussed in Theodorescu et al. (2023). The 204 identified ASVs belonged to Archaea (1) and to Bacteria (the rest). *Pseudomonadota* (65 %) was by far the most abundant phylum, represented by *Gammaproteobacteria* (62 %), followed by *Patescibacteria* (18 %), with the best represented *Saccharimonadia* class (10 %) (Fig. 2b). The most abundant genus was *Pseudomonas*, followed by 10 unassigned genera.

The water samples with 494 Bacteria ASVs and 5 Archaea ASVs had *Pseudomonadota* and *Bacteroidota* as the most abundant phyla in all samples (mean values 54 % and 15 %, respectively), like abundances in sediments (Fig. 2d). *Actinomycetota*, *Bacillota*, and an unassigned phylum followed. Like sediments, the best-represented classes in both samples were *Gammaproteobacteria* (mean value 41 %), *Alphaproteobacteria*, *Bacteroidia*, and an unassigned class (13 %–20 %). *Flavobacterium* was the dominant genus in the September samples, accounting for 15 %, with other genera, including *Pseudomonas* and *Acidivorax*, also present. The March sample had the most abundant unassigned genus belonging to an unassigned phylum.

Four ASVs of Archaea and 487 ASVs of Bacteria were identified in the dipluran microbiome. The most abundant phyla were *Pseudomonadota* (20 %–57 %), *Actinomycetota* (19 %–60 %), and *Bacillota* (9 %–29 %). *Actinobacteria* (18 %–59 %) were the most abundant class in all the studied individuals, followed by *Alphaproteobacteria*, *Gammaproteobacteria*, *Bacilli*, and *Clostridia*, which were abundant in one or more individuals. *Rickettsia* (~ 20 %) and *Paeniglutamibacter* (~ 15 %) were the most abundant genera (Fig. 2e).

Among *Archaea*, only a taxon was identified in both mirabilite samples, *Ca. Nitrocosmicus* that oxidises ammonia to nitrate, widely distributed in soils and other environments (Nicol et al., 2019). This archaeon was not identified in other samples. In sediments, only *Ca. Iainarchaeum*, *Methanobacterium*, and six other non-assigned genera were identified. *Ca. Iainarchaeum* and three non-assigned genera were identified in dipluran individuals, while water and moonmilk had only non-assigned genera.

3.2 Bacteria involved in the sulfur cycle

Pseudomonas, which can be involved in removing sulfur from organic compounds, was the dominant genus in mirabilite (55 %) and moonmilk (56 %). It was also second in abundance in water (3 %–8 %) and the dipluran microbiome (0.4 %–16 %). Mirabilite also contained *Rhodococcus* (~0.2 %). The sediments contained these genera in small abundances (<0.6 %). No other sulfur cycle-involved bacteria were identified in the mirabilite samples.

Sediments also contained in Station 1 (TS1), near the mirabilite heap, *Desulfovibrio* and *Bilophila* (each ~0.08 %); both are sulphate-reducing bacteria. *Desulfobacterota* also had very low abundances (~0.003 %) in STS1 and STS2. Very small amounts of other bacteria involved in the sulfur cycle were identified in moonmilk, like *Ectothiorhodospiraceae* and *Desulfobacterota* (both ~0.005 %). The *Ectothiorhodospiraceae* produce sulfur globules outside their cells (Garrity, 2005), classified as slightly halophilic, and *Desulfobacterota* is a sulfate-reducing phylum.

In the dipluran microbiome, one individual in Station 2 (TS2) had very low abundances of *Desulfovibrio* (0.02 %) and other unassigned *Desulfovibrionaceae* genera. An unassigned *Desulfobacterota* class was present in three of the sampled individuals at very low abundances.

3.3 Comparison between mirabilite and the other sample types

Differences among the samples in the Chao1 and Shannon indices (Fig. S1) indicated the lowest species richness in the mirabilite samples compared with the other samples, whereas the Shannon index showed high species distribution unevenness in the mirabilite, moonmilk, and STS1sep samples.

Pseudomonadota was dominant in mirabilite and all the other samples, with the co-dominance of *Actinomycetota* in mirabilite, *Bacteroidota* in most sediments (together with *Gemmatimonadota*) and water samples, and *Bacillota* with *Actinobacteriota* in diplurans (Fig. 3a). The dominant class in all samples was *Gammaproteobacteria*, with one dipluran individual as an exception (Fig. 3b). In sediments, *Bacteroida* and *Longimicrobia* were the co-dominant classes, and several classes were co-dominant in diplurans. Differences were

most obvious at the genus level, as explained in the description above, with clearer visualisation in Fig. 3c.

The Venn diagram (Fig. 3d) showed that mirabilite has 19 unique genera and an additional 17 shared with the sediments, as mirabilite samples also included small amounts of sediments from the heap. Five genera were shared with water samples, 9 with diplurans, and none with moonmilk.

In the PCA variable space (32 % total variation; Fig. 3e), the mirabilite and sediment samples are aligned along the F2 axis, and so was the moonmilk sample. The dipluran individuals were separated along the same axis, while both water samples were well separated from all other samples along the F1 axis.

The dendrogram of bacteria genus dissimilarity (Fig. 3f) more clearly shows the two main clusters, which are significantly separated, with the water samples in one cluster and the other samples, which are dissimilar to them, in the other cluster at a lower significance level. The moonmilk and the diplurans form separate subclusters. At the lowest dissimilarity, mirabilite clusters with the sediment in Station 1 in September and are dissimilar from all the other sediment samples.

3.4 Chemical comparison of the samples

Dripping water sample (WTS4) had a slightly alkaline pH (7.8 in March and 9.0 in September) and a low EC of ~100 $\mu\text{S cm}^{-1}$. The concentration of Ca was about 20 mg L^{-1} , whereas S was 2 mg L^{-1} , and K, Na and Mg were about 1 mg L^{-1} in both seasons. The other elements were present only in trace amounts (<10 $\mu\text{g L}^{-1}$). Water-soluble sulphate concentration varied widely among samples. The MTS2dec mirabilite had a very high (126 940 mg kg^{-1}) water-soluble sulphate concentration, whereas MTS1dec mirabilite (24 578 mg kg^{-1}) and STS1sep sediment (12 633 mg kg^{-1}) had moderate concentrations, and the other samples had low (240–9883 mg kg^{-1}) concentrations. The moonmilk (MOTS) sample had a slightly alkaline pH (8.6), low EC (120 $\mu\text{S cm}^{-1}$) and its chemical composition was dominated by Ca (33.5 %), accompanied by low amounts of Al (0.2 %) and Mg, Fe, K, and P (<0.1 %). The total S concentration was low (216 mg kg^{-1}), with more than 99 % was in water-soluble form. Sediments contain about 3 %–7 % Ca, 0.8–1.2 % Al and 0.2–2.8 % Fe. The Na, Mg, K, and P concentrations were <1 %, while the trace elements (Mn, Co, Ni, Cu, Zn, and Pb) concentrations were <0.03 %. Total S concentration in the sediments varied widely (84–9887 mg kg^{-1}), with more than 90 % present in water-soluble form. The sediments' pH was around 8, and the EC ranged from 1400 to 6400 $\mu\text{S cm}^{-1}$. Generally, higher concentrations of Ca, Mg, and Fe were observed in samples collected in September than in those collected in March. In contrast, the other elements were comparable in the two seasons (Table S2, Fig. 4a). There is a slight difference in the elemental composition of the two mirabilite

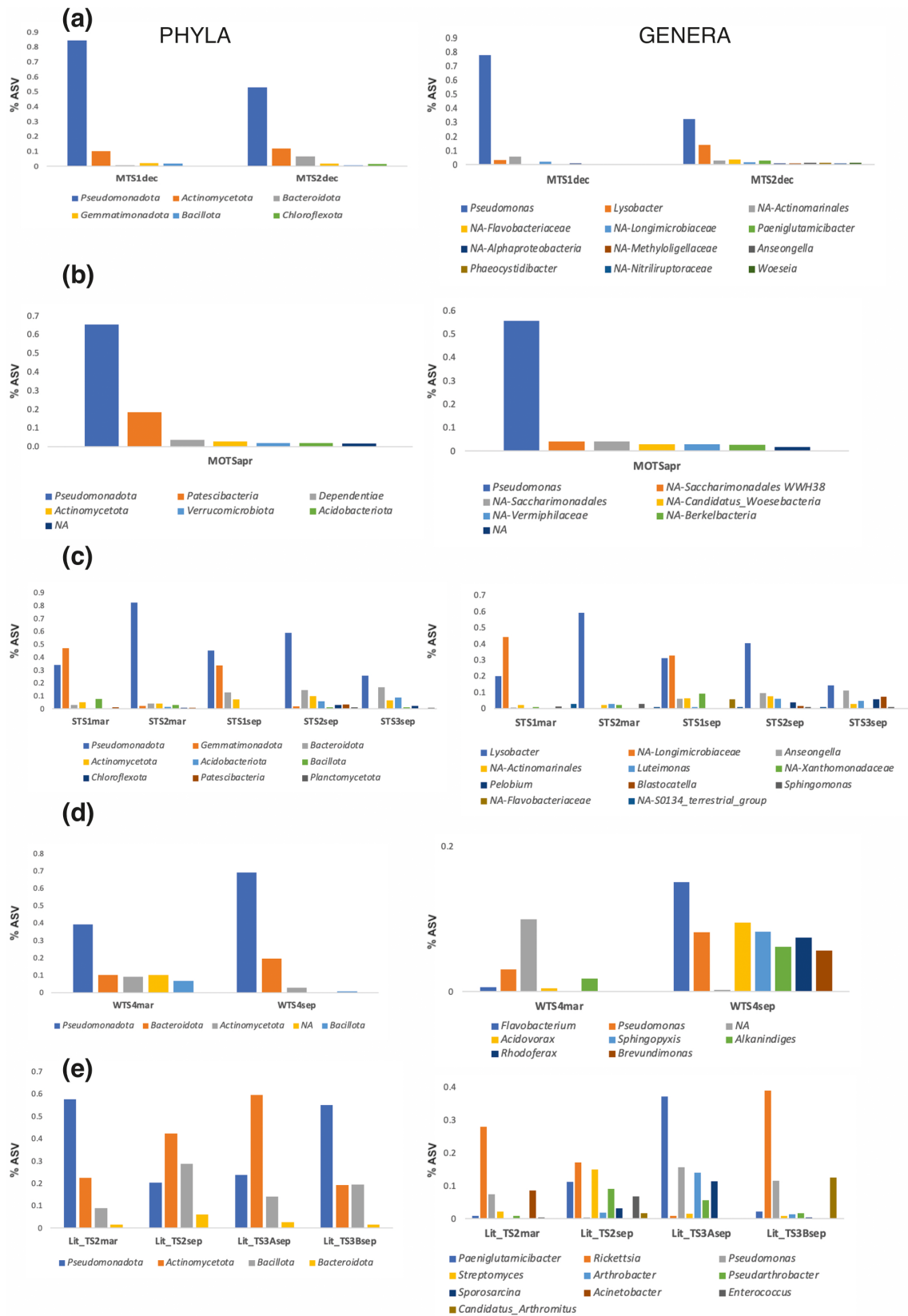


Figure 2. The most abundant bacteria phyla and genera in Tausoare Cave samples: mirabilite (a); moonmilk (b); sediment (c); water (d); dipluran (e). See Table 1 for abbreviations.

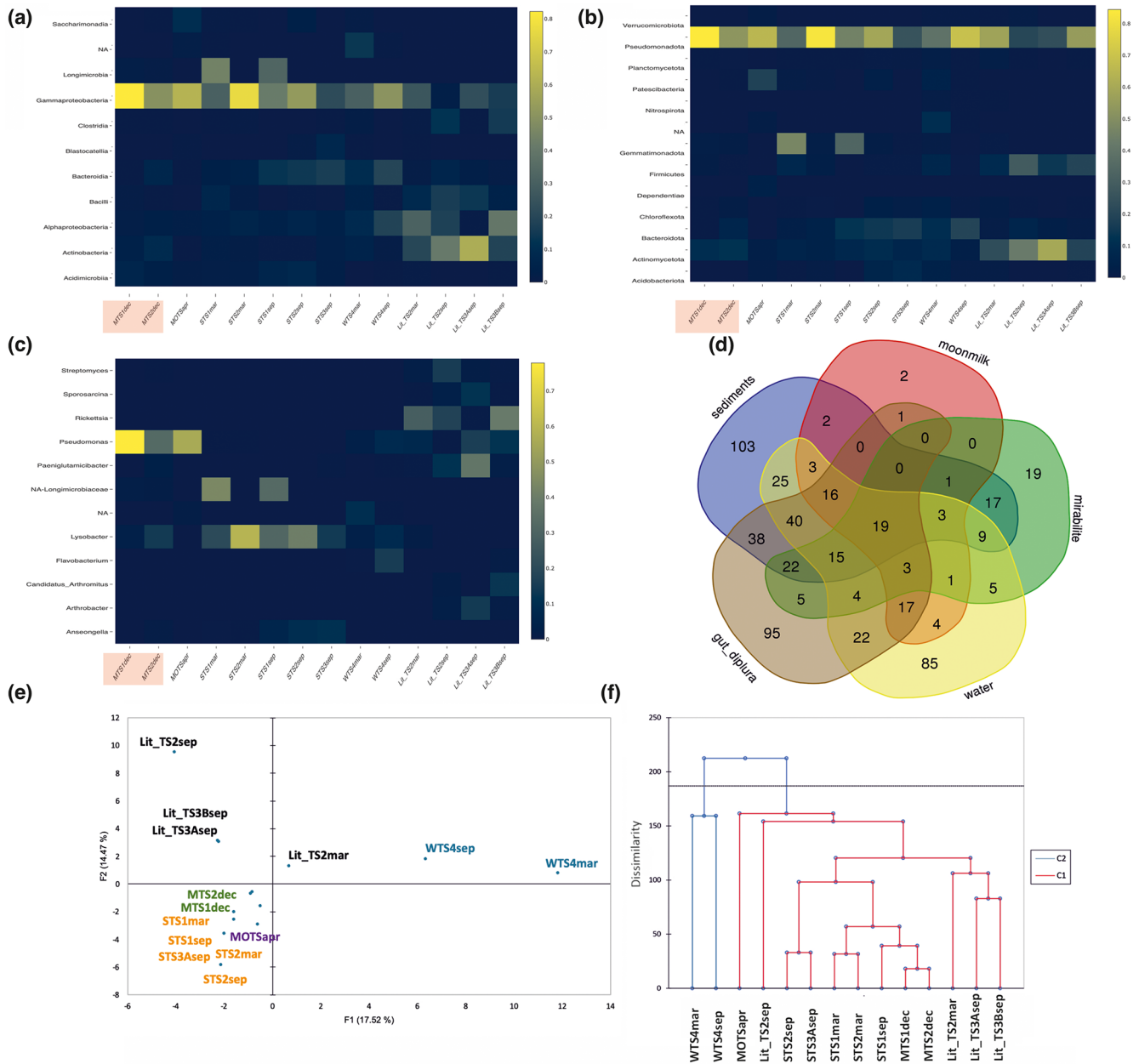


Figure 3. Differences between the bacteria in the analysed samples in Tausoare Cave, with the dominant phyla (a), classes (b), and genera (c) (y-axis) in each sample type (mirabilite samples marked with a red square); d. Venn diagram of the analysed samples at the genus level; e. PCA of the distribution of the most abundant bacteria genera in the variable space; f. Dendrogram showing the clustering of the samples by the most abundant bacteria genera. See Table 1 for abbreviations and Table S1 for the most abundant bacteria genera.

samples compared to the other. Both mirabilite samples have an alkaline pH. Na concentration was approximately 2-fold higher in MTS2dec, whereas the Al and Fe concentrations were approximately 5- and 15-fold lower than in MTS1dec. Although total S concentration in both mirabilite samples exceeded that of the sediment, it was about five times higher in MTS2dec than in MTS1dec. Nevertheless, the water-soluble fraction was about 95 % of the total sulfur in both samples. The MDS plot shows that the physicochemical parameters of

the moonmilk sample are significantly different from those of the other samples (Fig. S2). However, excluding the moonmilk sample from the MDS analysis (Fig. 4b) made the differences between the water, sediments, and mirabilite evident, as well as the distinction between the two mirabilite samples.

The FTIR spectrum of the MTS1dec mirabilite sample exhibits similar bands to those observed in MTS2dec, but the specific bands for sulphate are less intense, whereas those

of carbonate are more intense (more details in the Supplementary material and Fig. S3). The XRD data for MTS1dec confirm that quartz is the dominant phase, accompanied by albite, calcite, gypsum, and traces of thenardite. This is consistent with the lower concentration of soluble S measured in this sample (see the Supplementary material and Table S3 for more details).

4 Discussion

We approached the metabarcoding study of mirabilite in Tausoare Cave by including all the microbiomes from and around the heap containing this rare mineral. These elements comprised sediments from the mirabilite area and its immediate vicinity, as well as the microbiome of dipluran insects, which are typically abundant near the heaps. For comparison, we included the microbiomes of dripping water and moonmilk deposits from other cave passages. We hypothesised that the microbial community and metabolic activity associated with mirabilite could provide further insights into the conditions necessary for its formation at a specific location within the cave.

Different elemental distribution patterns were observed across the various sample types. Sodium, calcium, and sulfur are the predominant elements in the mirabilite samples, confirming the prominence of sodium sulphate, likely accompanied by calcium carbonate and calcium sulphate. The high iron content in one mirabilite (MTS1dec) sample is attributable to secondary minerals formed by the oxidation of pyrite. The moonmilk was completely separated from the other samples because its Ca content was one order of magnitude higher. This fact aligns with the known composition of moonmilk, which has calcium carbonate as the main mineral (Theodorescu et al., 2023). Bacteria composition showed a somewhat different pattern across all samples, with water and moonmilk separating from the other samples. Mirabilite, sediment, and dipluran microbiomes were broadly similar in dominant phyla and classes, with differences at the genus level.

The first and most striking observation from the bacterial diversity analysis was that no sulfur-reducing bacteria were identified in the mirabilite area of Tausoare Cave. *Desulfobacterota* and other sulfur cycle-related taxa were present in all the other sample types, although in low abundances. The absence of *Desulfobacterota* in the mirabilite samples is due to mirabilite formation, which involves sulfur and is sustained by the strong dominance of *Pseudomonas*. This bacterium uses organic sulfur sources, as evidenced by the sulfur-acquisition genes identified in its representatives (see the review by Scott et al., 2007). Recently, Xu et al. (2016) demonstrated that sulfide oxidation by a *Pseudomonas* species (C27) occurs in two stages. The first stage involves the formation of sulfur and the reduction of nitrate to nitrite, followed by the formation of thiosulfate via nitrite

reduction to N₂. Biooxidation of sulfide by *Pseudomonas* sp. C27 leads to the formation of either sulfur or thiosulfate, with the ratio of sulfide to nitrate concentrations significantly influencing the oxidation to the end products. At a ratio of 0.23, the conversion of sulfide to thiosulfate increased to ~ 100 %, but no thiosulfate was detected at a ratio of 2.7.

A similar pattern can be proposed for the formation of mirabilite in Tausoare Cave. The origin of sulfate in the mirabilite is from bituminous shale, resulting from the oxidation of pyrite and marcasite within the limestone body. However, it can also have a biotic origin, such as guano deposits (Wurster et al., 2015). In the Tables Room, a small colony of bats, numbering around 50 individuals, hibernates above the mirabilite heap. This colony is too small to represent a sulfide source, but it is enough to be one of ammonia, with the ammonia-oxidising Ca. *Nitrocosmicus* (Sauder et al., 2017) that was only present in the mirabilite samples (Fig. 5). The interaction between *Archaea* and *Bacteria* was already emphasised in sediments of a Chinese cave (Cheng et al., 2023). Another candidate for oxidising ammonia was *Nitrococcus*, found in the mirabilite and sediment samples at low abundances, though it was more abundant in the mirabilite. The presence of *Nitrococcus* can also be explained by its role in consuming nitrites. The small amount of ammonia the bats provide is sufficient to sustain an equilibrium microbial process that supports mirabilite growth in this cave (Fig. 5).

The high abundance of *Actinomycetota*, particularly in the mirabilite samples, which can grow extensive mycelia, can serve as scaffolds for the growth of mirabilite microfibers. For this study, we have not extracted fungi.

We could not identify a role for diplurans in the distribution and formation of mirabilite; however, their predominant occurrence around the heap area suggests they may be a limiting factor in mirabilite dispersal by consuming some of the microorganisms that contribute to its formation. They may also rely on certain sediment bacteria for nutrition, which are predominantly found in the Tables Room.

Mirabilite was first recorded in the Tausoare Cave after 1972, with a large distribution between 1986 and 1987, followed by a decline and a potential recovery in the last few decades (Silvestru, 1990, and personal observations). These changes were intended to be linked to adjustments in air circulation, including the opening of new passages within the caves and subsequent modifications to air circulation and local humidity in the Tables Room. High humidity is necessary to form and maintain this mineral, which requires 10 water molecules. Disruption of air circulation can be a limiting factor in mirabilite formation. However, as the temperature deep inside the cave is relatively constant and there is no air circulation in the Tables Room, we assumed this is not the case for changes in the arrangement of mirabilite inside the cave.

Personal observations also suggest that during some periods, when tourists visited the caves more frequently (even in very small numbers), mirabilite appeared in small patches outside the classical area. It is difficult to explain this “be-

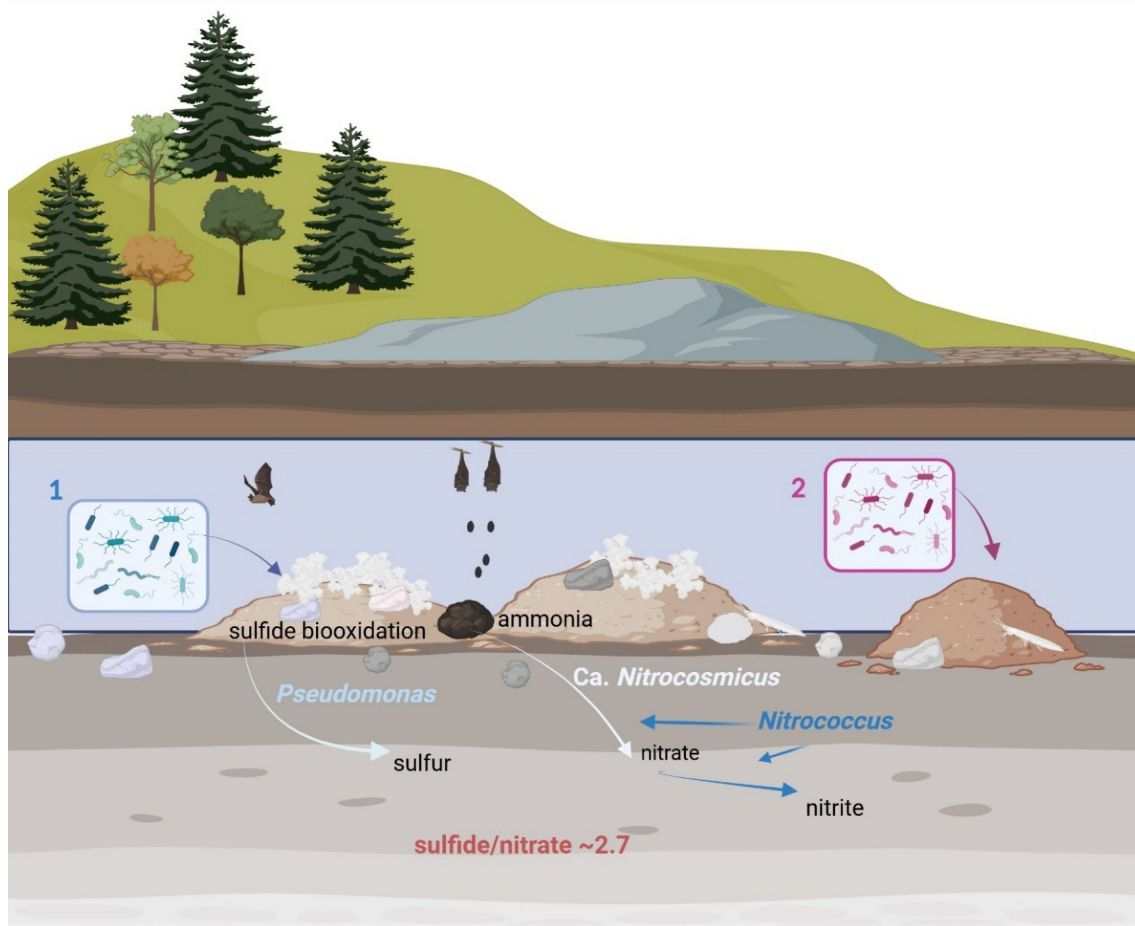


Figure 4. The chemical differences between the analysed samples from Tausoare Cave. (a) Concentration of chemical elements; (b) Two-dimensional MDS on the elemental concentration of mirabilite, water, and sediment samples. Kruskal's stress (1) = 0.042 indicates the significance of dissimilarity between samples. See Table 1 for abbreviations and Table S2 for the physicochemical characteristics. Created in <https://BioRender.com> (last access: 12 June 2026).

haviour" of a mineral if microorganisms are not considered and their role in creating the conditions for mirabilite formation is not acknowledged. Unfortunately, there are no data on the presence, absence, or numbers of bats prior to the 21st century.

Several limitations constrain the strength of these interpretations. First, the study relies primarily on only two mirabilite samples and their metabarcoding data, which provides taxonomic resolution but only indirect inference of metabolic activity; functional pathways are therefore hypothesised rather than directly demonstrated. Second, the absence of fungal community data is a significant gap, especially given fungi's potential structural and biogeochemical roles in mineral nucleation. Third, temporal variability – suggested by historical fluctuations in mirabilite distribution and tourism-related disturbances – was not systematically captured, limiting the ability to establish causal relationships between environmental changes and microbial dynamics. Additionally, the role of diplurans remains speculative, as no direct trophic or func-

tional interactions were experimentally validated. Finally, key environmental parameters, such as microscale humidity gradients and precise ammonia fluxes, were not quantitatively monitored, further limiting mechanistic interpretation.

Future work integrating metagenomics or metatranscriptomics, controlled geochemical measurements, and longitudinal sampling would be essential for validating the proposed microbial processes and more rigorously defining the biotic–abiotic feedback governing mirabilite formation in cave environments.

5 Conclusions

This integrative metabarcoding survey provides a still preliminary framework linking microbial community structure to mirabilite occurrence in the Tables Room of Tausoare Cave. The co-occurrence of sodium–sulfate-rich mineral assemblages with microbiomes dominated by *Pseudomonas*,

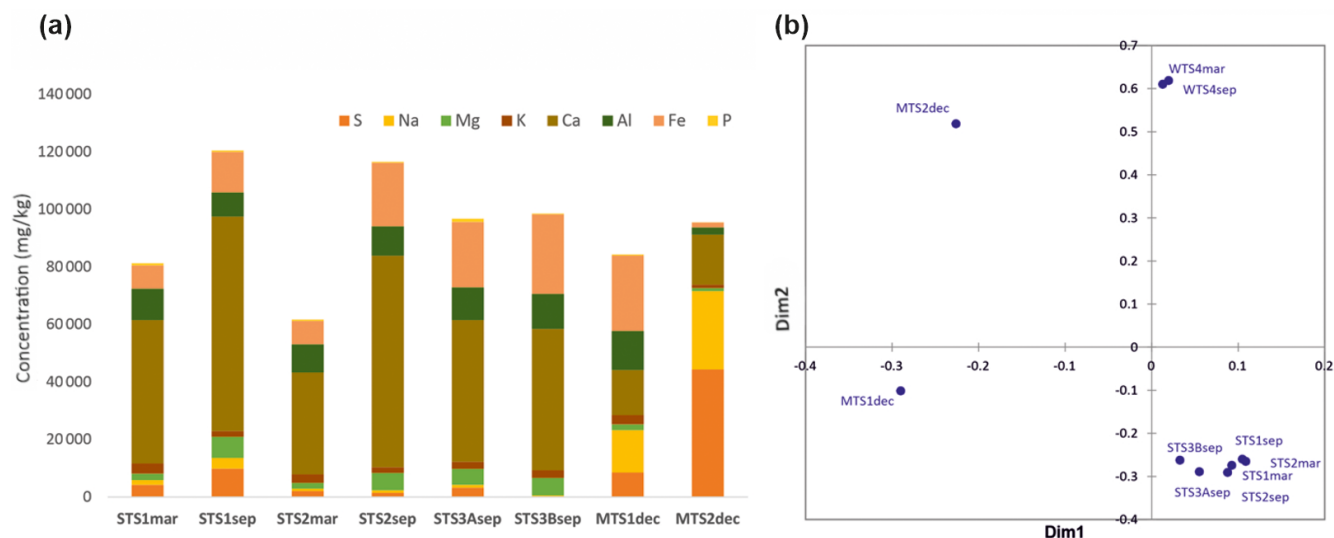


Figure 5. The schematic representation of the Tables Room in Tausoare Cave with mirabilite (1) and sediments (2) specific microbiomes. An equilibrium between sulfide originating from the rock and ammonia supplied by bats supports microorganisms that create conditions for mirabilite formation, which is promoted by *Pseudomonas*.

ammonia-oxidising archaea, and *Actinomycetota* supports the hypothesis that mirabilite formation is not purely physicochemical but instead emerges from a finely balanced interplay between geochemical inputs and microbial metabolism. In particular, the proposed coupling between sulfide oxidation, limited ammonia availability from bat activity, and microbial mediation offers a plausible explanation for the localised and dynamic nature of mirabilite formation in this cave.

We also presume that intermicrobial relationships are much more complex than those we observed from abundant and unique taxa in the mirabilite samples from Izvorul Tăușoarelor Cave. At this stage, we were able to provide new insights into the formation of mirabilite, as the dominance of *Pseudomonas* and the presence of an archaeon were observed only in the mirabilite samples.

The relationship between the mineral kingdom and microorganisms is a domain of interest due to its numerous applications (Konhauser and Alessi, 2024); however, it remains insufficiently recognised owing to the limited number of comprehensive studies on mineral formation. Consequently, we propose using the term “microbiocosm” to examine the complex interactions among microbes, encompassing all living and non-living components of the microbiomes surrounding a mineral environment. This term may elucidate the processes underlying mineral formation and enhance our understanding of the intricate interactions at the microscopic level.

Data availability. Sequence data generated in this study have been deposited in the European Nucleotide Archive (ENA) under the ac-

cession number PRJEB63212 for moonmilk and the rest of the samples in the National Centre for Biotechnology Information (NCBI) under accession number PRJNA1259755.

Supplement. The supplement related to this article is available online at <https://doi.org/10.5194/bg-23-4213-2026-supplement>.

Author contributions. OTM: concept, design, and writing of the manuscript; CTT: sampling and site description; EAL: sediment chemical analysis and interpretation; OC: XRD analysis and interpretation; all the authors corrected and approved the manuscript.

Competing interests. The contact author has declared that none of the authors has any competing interests.

Disclaimer. Publisher’s note: Copernicus Publications remains neutral with regard to jurisdictional claims made in the text, published maps, institutional affiliations, or any other geographical representation in this paper. The authors bear the ultimate responsibility for providing appropriate place names. Views expressed in the text are those of the authors and do not necessarily reflect the views of the publisher.

Acknowledgements. We thank Alexandru Petculescu for the climatic data, Mihail Theodorescu, Valentin Kiss, Cristian Sitar, and Marius Kenezs for their help with the sampling, and Ruxandra Bucur and Paul Adrian Bulzu for their help with the extractions and bioinformatics.

Financial support. This study received funding from a grant from the Ministry of Research and Innovation, CNCS – UEFISCDI, project number PN-III-P4-ID-PCCF-2016-0016 (DARKFOOD), within PNCD III. EAL was funded by the European Union Next Generation EU through the National Recovery and Resilience Plan, Component 9. I8., grant number 760104/May 23, 2023, code CF 245/November 29, 2022. This work was also supported by the project “Sensing, Mapping, Interconnecting: Tools for soil functions and services evaluation,” funded by the Romanian Government, Ministry of Innovation and Digitization, through the National Recovery and Resilience Plan (PNRR), PNRR-III-C9-2022-18, contract no. CF245/29.11.2022.

Review statement. This paper was edited by Pierre Amato and reviewed by two anonymous referees.

References

- Akacin, I., Ersoy, Ş., Doluca, O., and Güngörmüşler, M.: Comparing the significance of the utilization of next generation and third generation sequencing technologies in microbial metagenomics, *Microbiol. Res.*, 264, 127154, <https://doi.org/10.1016/j.micres.2022.127154>, 2022.
- Azzaro, M., Papale, M., Rizzo, C., Forte, E., Lenaz, D., Guglielmin, M., and Lo Giudice, A.: Antarctic Salt-Cones: An Oasis of Microbial Life? The Example of Boulder Clay Glacier (Northern Victoria Land), *Microorg.*, 10, 1753, <https://doi.org/10.3390/microorganisms10091753>, 2022.
- Banks, E. D., Taylor, N. M., Gully, J., Lubbers, B. R., Giarrizzo, J. G., Bullen, H. A., Hoehler, T. M., and Barton, H. A.: Bacterial Calcium Carbonate Precipitation in Cave Environments: A Function of Calcium Homeostasis, *Geomicrobio. J.*, 27, 444–454, <https://doi.org/10.1080/01490450903485136>, 2010.
- Barton, H. A. and Northup, D. E.: Geomicrobiology in cave environments: past, current and future perspectives, *J. Cave Karst. Stud.*, 69, 163–178, 2007.
- Baskar, S., Baskar, R., and Routh, J.: Biogenic evidences of moonmilk deposition in the Mawmluh Cave, Meghalaya, India, *Geomicrobio. J.*, 28, 252–265, 2011.
- Battler, M. M., Osinski, G. R., and Banerjee, N. R.: Mineralogy of saline perennial cold springs on Axel Heiberg Island, Nunavut, Canada and implications for spring deposits on Mars, *Icarus*, 224, 364–381, <https://doi.org/10.1016/j.icarus.2012.08.031>, 2013.
- Bazylnski, D. A., Frankel, R. B., and Konhauser, K. O.: Modes of biomineralization of magnetite by microbes, *Geomicrobio. J.*, 24, 465–475, <https://doi.org/10.1080/01490450701572259>, 2007.
- Callahan, B. J., McMurdie, P. J., Rosen, M. J., Han, A. W., Johnson, A. J. A., and Holmes, S. P.: DADA2: high-resolution sample inference from Illumina amplicon data, *Nat. Methods*, 13, 581–583, 2016a.
- Callahan, B. J., Sankaran, K., Fukuyama, J. A., McMurdie, P. J., and Holmes, S. P.: Bioconductor workflow for microbiome data analysis: from raw reads to community analyses, *F1000Research*, 5, 1492, <https://doi.org/10.12688/f1000research.8986.2>, 2016b.
- Canaveras, J. C., Cuezva, S., Sanchez-Moral, S., Lario, J., Laiz, L., Gonzalez, J. M., and Saiz-Jimenez, C.: On the origin of fiber calcite crystals in moonmilk deposits, *Naturwissenschaften*, 93, 27–32, 2006.
- Cheng, X., Xiang, X., Yun, Y., Wang, W., Wang, H., and Bodelier, P. L. E.: Archaea and their interactions with bacteria in a karst ecosystem, *Front. Microbiol.*, 14, 1068595, <https://doi.org/10.3389/fmicb.2023.1068595>, 2023.
- De Mandal, S., Panda, A. K., Bisht, S. S., and Kumar, N. S.: Microbial ecology in the era of next generation sequencing, *Next Generat. Sequenc. Appl.*, <https://doi.org/10.4172/2469-9853.s1-001>, 2015.
- Dhami, N. K., Mukherjee, A., and Watkin, E. L.: Characterisation of mineralogical-mechanical-microbial properties of calcitic speleothems and the in vivo biomineralization potential of associated microbial communities, *Front. Microbiol.*, 9, 40, <https://doi.org/10.3389/fmicb.2018.00040>, 2018.
- Garrity, G. M.: *Bergey’s Manual of Systematic Bacteriology, Volume 2: The Proteobacteria, Part B: The Gammaproteobacteria*, Springer, New York, <https://doi.org/10.1007/0-387-28022-7>, 2005.
- Gill, K. K., Jagniecki, E. A., Benison, K. C., and Gibson, M. E.: A Mars-analog sulfate mineral, mirabilite, preserves biosignatures, *Geology*, 51, 818–822, <https://doi.org/10.1130/G51256.1>, 2023.
- Haidău, C., Năstase-Bucur, R., Bulzu, P., Levei, E., Cadar, O., Mirea, I. C., Faur, L., Fruth, V., Atkinson, I., Constantin, S., and Moldovan, O. T.: A 16S rRNA Gene-Based Metabarcoding of Phosphate-Rich Deposits in Muierilor Cave, South-Western Carpathians, *Front. Microbiol.*, 13, <https://doi.org/10.3389/fmicb.2022.877481>, 2022.
- Herlemann, D. P., Labrenz, M., Jürgens, K., Bertilsson, S., Waniek, J. J., and Andersson, A. F.: Transitions in bacterial communities along the 2000 km salinity gradient of the Baltic Sea, *ISME J.*, 5, 1571–1579, 2011.
- Hershey, O. S. and Barton, H. A.: The microbial diversity of caves, in: *Cave ecology*, edited by: Moldovan, O. T., Kovác, L., and Hals, S., Cham: Springer Nature Switzerland, https://doi.org/10.1007/978-3-319-98852-8_5, 2018.
- Hill, J. C.: Johann Glauber’s discovery of sodium sulfate – Sal Mirabile Glauberi, *J. Chem. Edu.*, 56, 593, <https://doi.org/10.1021/ed056p593>, 1979.
- Hoffmann, T. D., Reeksting, B. J., and Gebhard, S.: Bacteria-induced mineral precipitation: a mechanistic review, *Microbiol. (Reading)*, 167, 001049, <https://doi.org/10.1099/mic.0.001049>, 2021.
- Howarth, F. G. and Moldovan, O. T.: Where Cave Animals Live, in: *Cave Ecology*, edited by: Moldovan, O. T., Kovac, L., and Halse, S., Springer International Publishing, ISBN 978-3-319-98852-8, 2018.
- Konhauser, K. and Alessi, D.: Geomicrobiology: Present Approaches and Future Directions, in: *Geomicrobiology: Natural and Anthropogenic Settings*, edited by: Staicu, L. C. and Barton, L. L. Springer, Cham, https://doi.org/10.1007/978-3-031-54306-7_1, 2024.
- Koning, K., McFarlane, R., Gosse, J. T., Lawrence, S., Carr, L., Horne, D., Van Wagoner, N., Boddy, C. N., and Cheeptham, N.: Biomineralization in Cave Bacteria-Popcorn and Soda Straw Crystal Formations, Morphologies, and Potential Metabolic Pathways, *Front. Microbiol.*, 13, 933388, <https://doi.org/10.3389/fmicb.2022.933388>, 2022.

- Krätner, H. G., Krätner, F. L., Szász, L., and Seghedi, I.: Geologic map of Romania, Rebra Sheet (20c). Scale 1:50.000, Inst Geol Geofiz, București, 1989.
- Lange-Enyedi, N. T., Németh, P., Borsodi, A. K., Spötl, C., and Makk, J.: Calcium carbonate precipitating extremophilic bacteria in an Alpine ice cave, *Sci. Rep.*, 14, 2710, <https://doi.org/10.1038/s41598-024-53131-y>, 2024.
- Marliacy, P., Solimando, R., Bouroukba, M., and Schuffenecker, L.: Thermodynamics of crystallization of sodium sulfate decahydrate in H_2O – NaCl – Na_2SO_4 : application to $\text{Na}_2\text{SO}_4 \cdot 10\text{H}_2\text{O}$ -based latent heat storage materials, *Thermochim. Acta*, 344, 85–94, [https://doi.org/10.1016/S0040-6031\(99\)00331-7](https://doi.org/10.1016/S0040-6031(99)00331-7), 2000.
- Martin, M.: Cutadapt removes adapter sequences from high-throughput sequencing reads, *EMBnet.journal*, 17, 10–12, 2011.
- McMurdie, P. J. and Holmes, S.: Phyloseq: An R Package for Reproducible Interactive Analysis and Graphics of Microbiome Census Data, *PLoS ONE*, 8, e61217, <https://doi.org/10.1371/journal.pone.0061217>, 2013.
- Meka, A. F., Bekele, G. K., Abas, M. K., and Gameda, M. T.: Exploring microbial diversity and functional gene dynamics associated with the microbiome of Sof Umer cave, Ethiopia, *Discov. Appl. Sci.*, 6, 400, <https://doi.org/10.1007/s42452-024-06110-x>, 2024.
- Möhlmann, D. and Thomsen, K.: Properties of cryobrines on Mars, *Icarus*, 212, 123–130, <https://doi.org/10.1016/j.icarus.2010.11.025>, 2011.
- Mulder, S. J., van Ruitenbeek, F. J. A., Foing, B. H., and Sánchez-Román, M.: Multitechnique characterization of secondary minerals near HI-SEAS, Hawaii, as Martian subsurface analogues, *Sci. Rep.*, 13, 22603, <https://doi.org/10.1038/s41598-023-48923-7>, 2023.
- Nicol, G. W., Hink, L., Gubry-Rangin, C., Prosser, J. I., and Lehtovirta-Morley, L. E.: Genome Sequence of "Candidatus *Nitrosocosmicus franklandus*" C13, a Terrestrial Ammonia-Oxidizing Archaeon, *Microbiol. Resour. Announc.*, 8, e00435-19, <https://doi.org/10.1128/MRA.00435-19>, 2019.
- Northup, D. E. and Lavoie, K. H.: Geomicrobiology of caves: a review, *Geomicrobiol. J.*, 18, 199–222, 2001.
- Onac, B. P., Drăgușin, V., Papiu, F., and Theodorescu, C. T.: Rodna Mountains: Izvorul Tăușoarelor Cave (Pestera de la Izvorul Tăușoarelor), in: Cave and Karst Systems of Romania. Cave and Karst Systems of the World, edited by: Ponta, G. and Onac, B., Springer, Cham, https://doi.org/10.1007/978-3-319-90747-5_7, 2019.
- Pruesse, E., Quast, C., Knittel, K., Fuchs, B. M., Ludwig, W., Peplies, J., and Glöckner, F. O.: SILVA: a comprehensive online resource for quality checked and aligned ribosomal RNA sequence data compatible with ARB, *Nucleic Acids Res. Spec. Publ.*, 35, 7188–7196, 2007.
- Puławska, A., Kalinowska, J., Rachubik, M., Drzewiecka, D., Albuquerque, L., Egas, C., Krawczyk, K., Manecki, M., Loch, C., and Kowalewicz-Kulbat, M.: Halophilic and Non-Halophilic Microbial Communities in Relation to Physico-Chemical Characteristics of Salt Mine Air, *Environ. Microbiol. Rep.*, 17, e70095, <https://doi.org/10.1111/1758-2229.70095>, 2025.
- Samanta, B., Sharma, S., and Budhwar, R.: Metagenome analysis of speleothem microbiome from Subterranean Cave reveals insight into community structure, metabolic potential, and BGCs diversity, *Curr. Microbiol.*, 80, 317, <https://doi.org/10.1007/s00284-023-03431-9>, 2023.
- Sauder, L., Albertsen, M., Engel, K., Schwarz, J., Nielsen, P. H., Wagner, M., and Neufeld, J. D.: Cultivation and characterization of *Candidatus Nitrosocosmicus exaquare*, an ammonia-oxidizing archaeon from a municipal wastewater treatment system, *ISME J.*, 11, 1142–1157, <https://doi.org/10.1038/ismej.2016.192>, 2017.
- Scott, S., Hilton, M. E., Coppin, C. W., Russell, R. J., Oakeshott, J. G., and Sutherland, T. D.: A global response to sulfur starvation in *Pseudomonas putida* and its relationship to the expression of low-sulfur-content proteins, *FEMS Microbiol. Lett.*, 267, 184–193, <https://doi.org/10.1111/j.1574-6968.2006.00575.x>, 2007.
- Shen, J., Smith, A. C., Barnett, M. J., Morgan, A., and Wynn, P. M.: Distinct microbial communities in the soils, waters, and speleothems of a hyperalkaline cave system, *J. Geophys. Res.-Biogeo.*, 127, e2022JG006866, <https://doi.org/10.1029/2022jg006866>, 2022.
- Silvestru, E.: On the genesis and evolution of mirabilite in the cave of Izvorul Tăușoarelor (Romania), *Trav. Inst. Speol. "E. Racovitza"*, 29, 79–83, 1990.
- Silvestru, E. and Viehmann, I.: Étude de microtectonique comparée dans le Karst des Monts Rodna (Roumanie), *Trav. Inst. Speol. "E. Racovitza"*, 21, 63–67, 1982.
- Tao, L., Fu, J., Wang, F., Song, Y., Li, Y., Zhang, J., and Wang, Z.: The application of mirabilite in traditional Chinese medicine and its chemical constituents, processing methods, pharmacology, toxicology and clinical research, *Front. Pharmacol.*, 14, 1293097, <https://doi.org/10.3389/fphar.2023.1293097>, 2024.
- Theodorescu, M., Bucur, R., Bulzu, P. A., Faur, L., Levei, E. A., Mirea, I. C., Cadar, O., Ferreira, R., Souza-Silva, M., and Moldovan, O. T.: Environmental Drivers of the Moonmilk Microbiome Diversity in Some Temperate and Tropical Caves, *Microb. Ecol.*, 86, 2847–2857, 2023.
- Viehmann, I., Rusu, T., and Șerban, M.: Complexul carstic Tăușoare-Zalion (Munții Rodnei), *Lucr. Inst. Speol. "E. Racovitza"*, 3, 21–48, 1964.
- White, W. B.: Secondary minerals in volcanic caves: data from Hawai'i, *J. Cave Karst Stud.*, 72, 75–85, 2010.
- White, W. B.: Mineralogy of Mammoth Cave, in: Mammoth Cave: A Human and Natural History. Cave and Karst Systems of the World, edited by: Hobbs III, H. H., Olson, R. A., Winkler, E. G., and Culver, D. C., Cham, Switzerland: Springer International Publishing, https://doi.org/10.1007/978-3-319-53718-4_9, 2017.
- White, W. B.: Chapter 59 – Gypsum flowers and related speleothems, in: *Encyclopedia of Caves (Third Edition)*, edited by: White, W. B., Culver, D. C., and Pipan, T., Academic Press, <https://doi.org/10.1016/C2017-0-01162-X>, 2019.
- Wurster, C. M., Munksgaard, N., Zwart, C., and Bird, M.: The biogeochemistry of insectivorous cave guano: A case study from insular Southeast Asia, *Biogeochem.*, 124, 163–175, <https://doi.org/10.1371/journal.pone.0230865>, 2015.
- Xu, X. J., Chen, C., Guo, H.-l., Wang, A.-j., Ren, N.-Q., and Lee, D.-J.: Characterization of a newly isolated strain *Pseudomonas* sp. C27 for sulfide oxidation: Reaction kinetics and stoichiometry, *Sci. Rep.*, 6, 21032, <https://doi.org/10.1038/srep21032>, 2016.
- Zhu, H. Z., Jiang, C. Y., and Liu, S. J.: Microbial roles in cave biogeochemical cycling, *Front. Microbiol.*, 13, 950005, <https://doi.org/10.3389/fmicb.2022.950005>, 2022.

Zhu, H. Z., Zhang, Z. F., Zhou, N., Jiang, C., Wang, B., Cai, L., Wang, H., and Liu, S.: Bacteria and metabolic potential in Karst Caves revealed by intensive bacterial cultivation and genome assembly, *Appl. Environ. Microbiol.*, 87, <https://doi.org/10.1128/aem.02440-20>, 2021.